Decomposed Lifting-Line Predictions and Optimization for Propulsive Efficiency of Flapping Wings

W. F. Phillips* and R. A. Miller†
Utah State University, Logan, Utah 84322-4130

and

D. F. Hunsaker‡
Scaled Composites, Mojave, CA 93501-1663

A decomposed Fourier series solution to Prandtl's classical lifting-line theory is used to predict the lift, induced-thrust, and power coefficients developed by a flapping wing. A significant advantage of this quasi-steady analytical solution over commonly used numerical methods is the utility provided for optimizing wing flapping cycles. The analytical solution involves five time-dependent functions that could all be optimized to maximize thrust, propulsive efficiency, and/or other performance measures. Results show that by optimizing only two of these five functions, propulsive efficiencies exceeding 97% can be obtained. Results are presented for untwisted rectangular wings in pure plunging, rectangular wings with linear washout and the minimum-power washout magnitude, and rectangular wings with the minimum-power washout distribution and magnitude.

Nomenclature

A_n = Fourier coefficients in the series solution to the lifting-line equation
a_n = planform coefficients in the decomposed Fourier series solution to the lifting-line equation
b = wingspan
b_n = washout coefficients in the decomposed Fourier series solution to the lifting-line equation
C_{Di} = instantaneous wing induced-drag coefficient
$\overline{C}_{Di}$ = mean wing induced-drag coefficient averaged over a complete flapping cycle
C_{D_p} = wing parasitic-drag coefficient
C_L = instantaneous wing lift coefficient
$\overline{C}_L$ = mean wing lift coefficient averaged over a complete flapping cycle
C_{LA} = sinusoidal amplitude for the wing lift coefficient
$C_{L,\alpha}$ = wing lift slope, Eq. (15)
$\widetilde{C}_{L,\alpha}$ = airfoil-section lift slope
$\overline{C}_{P_A}$ = mean available-power coefficient averaged over a complete flapping cycle
C_{P_f} = instantaneous flapping-power coefficient required to support the flapping rate p
$\overline{C}_{P_f}$ = mean flapping-power coefficient averaged over a complete flapping cycle
$C_0 - C_2$ = optimization coefficients, Eqs. (53)–(55)
c = local wing section chord length
D = wing drag

* Professor, Mechanical and Aerospace Engineering Department, 4130 Old Main Hill. Senior Member AIAA.
† Undergraduate Student, Mechanical and Aerospace Engineering Department, 4130 Old Main Hill. Member AIAA.
‡ Design Engineer, 1624 Flight Line. Member AIAA.

d_n = plunging coefficients in the decomposed Fourier series solution to the lifting-line equation
E_n = plunging coefficients in the Fourier series solution for induced drag, Eq. (8)
e_n = plunging coefficients in the Fourier series solution for induced drag, Eq. (22)
$\widetilde{L}$ = local section lift
M = number of control points used to define a numerical twist distribution function
N = number of terms retained in a truncated infinite series
P_f = instantaneous power required to support the instantaneous flapping rate p
p = angular wingtip rotation rate about the midspan resulting from wing flapping
$\hat{p}$ = dimensionless angular wingtip rotation rate about the midspan resulting from wing flapping, $pb/(2V_\infty)$
$\hat{p}_{\text{rms}}$ = root mean square of the dimensionless flapping rate averaged over a complete flapping cycle
R_A = wing aspect ratio
R_O = optimization ratio, Eq. (51)
S = wing planform area
$\overline{T}_f$ = mean induced thrust developed by wing flapping
t = time
V_p = y component of relative wind resulting from airfoil-section plunging
V_∞ = freestream airspeed
W = weight
x, y, z = streamwise, upward normal, and spanwise coordinates relative to the quarter chord midspan
y_{ac} = y coordinate of the airfoil-section aerodynamic center located at the spanwise coordinate z
α = geometric angle of attack
α_{L0} = zero-lift angle of attack
Γ = wing section circulation
γ_t = strength of the trailing vortex sheet per unit span
$\Delta\alpha_p$ = spanwise variation in local angle of attack increment resulting from wing section plunging
η_p = mean propulsive efficiency averaged over a complete flapping cycle
θ = change of variables for the spanwise coordinate, Eq. (3)
κ_a = planform coefficient in the lifting-line relation for required power, Eq. (24)
κ_b = washout coefficient in the lifting-line relation for required power, Eq. (25)
κ_D = planform coefficient in the lifting-line relation for induced drag, Eq. (16)
κ_{DL} = washout–lift coefficient in the lifting-line relation for induced drag, Eq. (17)
$\kappa_{D\Omega}$ = washout coefficient in the lifting-line relation for induced drag, Eq. (18)
κ_d = plunging coefficient in the lifting-line relation for required power, Eq. (26)
κ_{Lp} = plunging–lift coefficient in the lifting-line relation for induced drag, Eq. (19)
κ_p = plunging coefficient in the lifting-line relation for induced drag, Eq. (21)
$\kappa_{\Omega p}$ = plunging–washout coefficient in the lifting-line relation for induced drag, Eq. (20)
ρ = air density
τ = sinusoidal period
ϕ = instantaneous flapping dihedral angle
ϕ_A = sinusoidal amplitude for the flapping dihedral angle
ψ = spanwise twist distribution function resulting from airfoil-section plunging
Ω = total symmetric wing washout angle, geometric plus aerodynamic
Ω_{opt} = optimum total symmetric wing washout angle, geometric plus aerodynamic
ω = spanwise twist distribution function resulting from symmetric wing washout

I. Introduction

PRANDTL'S classical lifting-line theory[1,2] can be used to obtain a solution for the spanwise distribution of section lift and induced drag generated on a finite wing. If the circulation about any spanwise section of the wing is $\Gamma(z)$ and the strength of the trailing vortex sheet per unit span is $\gamma_t(z)$, as shown in Fig. 1, then Helmholtz's vortex theorem and the Kutta–Joukowski law[3,4] produce the fundamental lifting-line equation, i.e.,

$$\frac{2\Gamma(z)}{V_\infty c(z)} + \frac{\widetilde{C}_{L,\alpha}}{4\pi V_\infty} \int_{\zeta=-b/2}^{b/2} \frac{1}{z-\zeta}\left(\frac{d\Gamma}{dz}\right)_{z=\zeta} d\zeta \;=\; \widetilde{C}_{L,\alpha}[\alpha(z)-\alpha_{L0}(z)] \tag{1}$$

In Eq. (1) α and α_{L0} are allowed to vary with the spanwise coordinate z to account for wing twist, control surface deflection, and airfoil-section plunging that may vary along the span. Neglecting the effects of sweep and dihedral, an analytical solution to Prandtl's lifting-line equation for a finite wing can be obtained in terms of a Fourier sine series. For a given wing geometry with a known spanwise distribution of relative wind, the planform shape, $c(z)$, the geometric angle of attack, $\alpha(z)$, and the zero-lift angle of attack, $\alpha_{L0}(z)$, are all known functions of the spanwise coordinate. The circulation distribution is written as a Fourier series, the series is truncated to a finite number of terms (N), and the Fourier coefficients are determined by forcing the lifting-line equation to be satisfied at N specific sections along the span of the wing. From this solution the circulation distribution is given by

$$\Gamma(\theta) \;=\; 2bV_\infty \sum_{n=1}^{N} A_n \sin(n\theta) \tag{2}$$

where θ is a change of variables for the spanwise coordinate defined as

$$\theta \;\equiv\; \cos^{-1}(-2z/b) \tag{3}$$

After substituting the circulation distribution specified by Eq. (2) into the lifting-line equation given by Eq. (1), the Fourier coefficients, A_n, are obtained from the relation

$$\sum_{n=1}^{N} A_n \left[\frac{4b}{\widetilde{C}_{L,\alpha}\, c(\theta)} + \frac{n}{\sin(\theta)}\right] \sin(n\theta) \;=\; \alpha(\theta)-\alpha_{L0}(\theta) \tag{4}$$

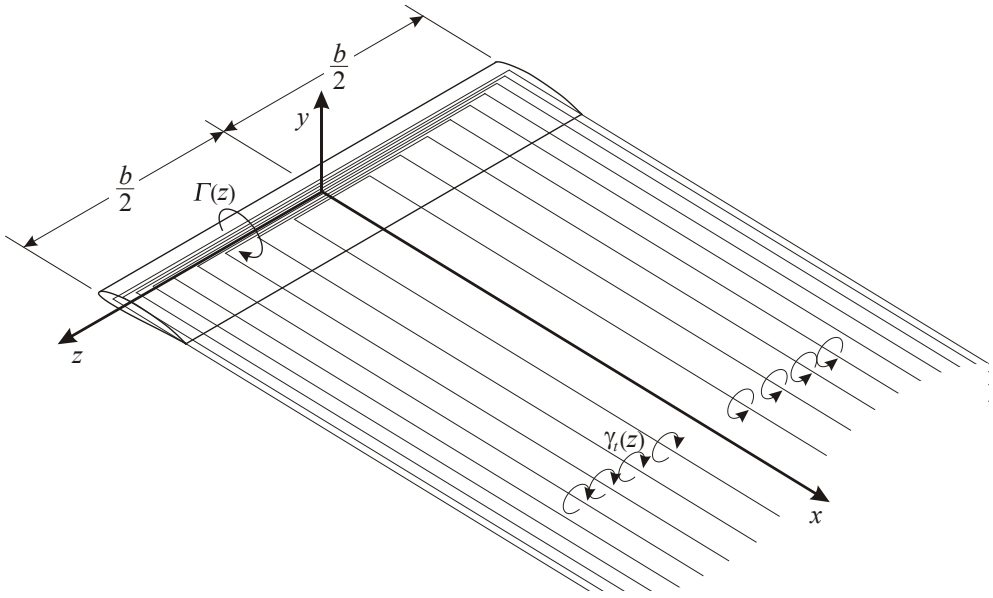

Figure 1. Prandtl's model for the section circulation and trailing vortex sheet generated by a finite wing.

Even in the presence of airfoil-section plunging that varies along the wingspan, the lift coefficient predicted by lifting-line theory can be obtained from the relation[5]

$$C_L = \pi R_A A_1 \tag{5}$$

where $R_A \equiv b^2/S$ is the wing aspect ratio. Airfoil-section plunging and wing twist that vary along the span of the wing can have a very significant effect on the induced drag predicted by lifting-line theory. The lifting-line relation developed by Phillips[5] for predicting the induced-drag coefficient in the presence of airfoil-section plunging can be written as

$$C_{D_i} = \pi R_A \sum_{n=1}^{N} n A_n^2 - \pi R_A \sum_{n=1}^{N} A_n E_n \tag{6}$$

or after applying Eq. (5)

$$C_{D_i} = \frac{C_L^2}{\pi R_A} + \pi R_A \sum_{n=2}^{N} n A_n^2 - \pi R_A \sum_{n=1}^{N} A_n E_n \tag{7}$$

where the coefficients E_n are obtained from

$$E_n \equiv \frac{2}{\pi} \int_{\theta=0}^{\pi} \frac{V_p(\theta)}{V_\infty} \sin(n\theta) \sin(\theta) d\theta \tag{8}$$

and $V_p(\theta)$ is the y component of relative wind resulting from airfoil-section plunging at the spanwise coordinate θ.

To prevent boundary layer separation, the local section geometric angle of attack must remain small at all spanwise sections of the wing. So in the absence of stall, the component of relative wind normal to the flight path that results from airfoil-section plunging must remain small compared to the freestream airspeed. Boundary layer separation must be avoided to maintain high lift-to-drag ratios in forward flight. Furthermore, within the small-angle approximation, wing dihedral has no effect on either lift or induced drag. Hence, for the flapping wings of some birds in high-speed forward flight and other flight phases where aerodynamic efficiency and endurance are of paramount importance, the lifting-line solution given by Eqs. (2)–(8) could be used.

During wing flapping the lift developed on the wing and the vorticity shed from the wing typically change periodically with time. Because the vortex sheet trailing aft of a lifting wing contains a time history of the vorticity shed from the wing, the strength of this trailing vortex sheet is not typically constant during wing flapping. Hence, because the trailing vortex sheet has a significant effect on the aerodynamic lift and drag, periodic variations in lift can have a significant effect on these forces as well. Because shed vorticity is carried away from the wing at the freestream airspeed, the effect of unsteady lift can be typically neglected during wing flapping when the freestream airspeed is large compared with the product of the wing chord length and the flapping frequency. A two-dimensional analytical solution first obtained by Theodorsen[6] for small-amplitude sinusoidal plunging of an airfoil shows that the two-dimensional effects of unsteady lift can be neglected when the product of the airfoil chord length and the plunging frequency divided by the freestream airspeed is on the order of 0.1 or less. Because the lifting-line solutions presented here are quasi-steady solutions, the flapping frequency must be low enough and the freestream airspeed must be high enough so that this condition is satisfied.[5]

For a finite wing with geometric and/or aerodynamic twist, the lifting-line solution expressed in the form of Eqs. (2)–(8) is cumbersome for the evaluation of traditional wing properties, because the Fourier coefficients depend on angle of attack and must be reevaluated for each operating condition studied. A more useful form of the lifting-line solution has been presented.[7–10] For flapping wings in the absence of control surface deflection, this lifting-line solution is based on decomposing the Fourier coefficients, A_n, using the simple change of variables[5]

$$A_n = a_n(\alpha - \alpha_{L0})_{\text{root}} - b_n \Omega + d_n \hat{p} \tag{9}$$

The three components on the right-hand side of Eq. (9) are, respectively, the contributions from the wing planform, geometric and/or aerodynamic washout, and airfoil-section rotation about the midspan resulting from wing flapping.

To satisfy Eq. (4) with the change of variables given in Eq. (9), the decomposed Fourier coefficients, a_n, b_n, and d_n, are evaluated from

$$\sum_{n=1}^{N} a_n \left[\frac{4b}{\widetilde{C}_{L,\alpha}\, c(\theta)} + \frac{n}{\sin(\theta)} \right] \sin(n\theta) \;=\; 1 \tag{10}$$

$$\sum_{n=1}^{N} b_n \left[\frac{4b}{\widetilde{C}_{L,\alpha}\, c(\theta)} + \frac{n}{\sin(\theta)} \right] \sin(n\theta) \;=\; \omega(\theta) \tag{11}$$

$$\sum_{n=1}^{N} d_n \left[\frac{4b}{\widetilde{C}_{L,\alpha}\, c(\theta)} + \frac{n}{\sin(\theta)} \right] \sin(n\theta) \;=\; \psi(\theta) \tag{12}$$

where the functions $\omega(\theta)$ and $\psi(\theta)$ are the spanwise variations in local section aerodynamic angle of attack resulting from unit amounts of wing washout and dimensionless rotation about the midspan, respectively. Similarly, the scalar variables $(\alpha - \alpha_{L0})_{\text{root}}$, Ω, and $\hat{p}$ are, respectively, the magnitudes of the root section aerodynamic angle of attack, wing washout, and dimensionless rotation rate about the wing midspan resulting from wing flapping. The variables $(\alpha - \alpha_{L0})_{\text{root}}$ and Ω are deflection angles in radians, and $\hat{p}$ is a dimensionless angular rate defined as $\hat{p} \equiv pb/(2V_\infty)$, where p is the magnitude of the wingtip rotation rate about the wing midspan. The function $\omega(\theta)$ is called the washout distribution function[10] and the function $\psi(\theta)$ is referred to as the plunging distribution function.[5]

For the small-angle wing flapping required to prevent stall in forward flight, the instantaneous lift and induced-drag coefficients can be predicted using Eqs. (5) and (7), and after applying Eq. (9) and rearranging we obtain[5]

$$C_L \;=\; \pi R_A [a_1(\alpha - \alpha_{L0})_{\text{root}} - b_1\Omega + d_1\hat{p}] \tag{13}$$

$$C_{D_i} = \frac{(1+\kappa_D)C_L^2 - \kappa_{DL} C_L C_{L,\alpha}\Omega + \kappa_{D\Omega}(C_{L,\alpha}\Omega)^2}{\pi R_A} + \frac{(-\kappa_{Lp} C_L + \kappa_{\Omega p} C_{L,\alpha}\Omega - \kappa_p C_{L,\alpha}\hat{p}) C_{L,\alpha}\hat{p}}{\pi R_A} \tag{14}$$

$$C_{L,\alpha} \;\equiv\; \pi R_A a_1 \tag{15}$$

$$\kappa_D \;\equiv \sum_{n=2}^{N} n \frac{a_n^2}{a_1^2} \tag{16}$$

$$\kappa_{DL} \;\equiv\; 2\frac{b_1}{a_1} \sum_{n=2}^{N} n \frac{a_n}{a_1} \left(\frac{b_n}{b_1} - \frac{a_n}{a_1} \right) \tag{17}$$

$$\kappa_{D\Omega} \;\equiv\; \left(\frac{b_1}{a_1} \right)^2 \sum_{n=2}^{N} n \left(\frac{b_n}{b_1} - \frac{a_n}{a_1} \right)^2 \tag{18}$$

$$\kappa_{Lp} \;\equiv\; \frac{e_1}{a_1} + \frac{d_1}{a_1} \sum_{n=2}^{N} \frac{a_n}{a_1} \left[\frac{e_n}{d_1} - 2n \left(\frac{d_n}{d_1} - \frac{a_n}{a_1} \right) \right] \tag{19}$$

$$\kappa_{\Omega p} \;\equiv\; \frac{b_1}{a_1}\frac{d_1}{a_1} \sum_{n=2}^{N} \left(\frac{b_n}{b_1} - \frac{a_n}{a_1} \right) \left[\frac{e_n}{d_1} - 2n \left(\frac{d_n}{d_1} - \frac{a_n}{a_1} \right) \right] \tag{20}$$

$$\kappa_p \;\equiv\; \left(\frac{d_1}{a_1} \right)^2 \sum_{n=2}^{N} \left(\frac{d_n}{d_1} - \frac{a_n}{a_1} \right) \left[\frac{e_n}{d_1} - n \left(\frac{d_n}{d_1} - \frac{a_n}{a_1} \right) \right] \tag{21}$$

$$e_n \;\equiv\; \frac{2}{\pi} \int_{\theta=0}^{\pi} \psi(\theta) \sin(n\theta) \sin(\theta)\, d\theta \tag{22}$$

The flapping-power coefficient is defined to be the required power input P_f divided by $\frac{1}{2}\rho V_\infty^3 S$, and for spanwise symmetric wings, the instantaneous flapping-power coefficient required to support the instantaneous symmetric flapping rate p as predicted by lifting-line theory is[5]

$$C_{P_f} \equiv \frac{P_f}{\frac{1}{2}\rho V_\infty^3 S} = 4(\kappa_a C_L - \kappa_b C_{L,\alpha}\Omega + \kappa_d C_{L,\alpha}\hat{p})\hat{p} \tag{23}$$

$$\kappa_a \equiv \frac{1}{3\pi} + \frac{1}{\pi}\sum_{n=3}^{N}\frac{(-1)^{(n+1)/2}}{n^2-4}\frac{a_n}{a_1}\bigg|_{\text{for } n \text{ odd}} \tag{24}$$

$$\kappa_b \equiv \frac{b_1}{\pi a_1}\sum_{n=3}^{N}\frac{(-1)^{(n+1)/2}}{n^2-4}\left(\frac{b_n}{b_1} - \frac{a_n}{a_1}\right)\bigg|_{\text{for } n \text{ odd}} \tag{25}$$

$$\kappa_d \equiv \frac{d_1}{\pi a_1}\sum_{n=3}^{N}\frac{(-1)^{(n+1)/2}}{n^2-4}\left(\frac{d_n}{d_1} - \frac{a_n}{a_1}\right)\bigg|_{\text{for } n \text{ odd}} \tag{26}$$

In its most general form, the periodic motion associated with wing flapping can be extremely complex. We know from slow-motion video that the wing flapping cycle of many birds can involve time-dependent spanwise variations in both twist and sweep, which are coordinated with the periodic flapping motion. Furthermore, because the wings of a bird are multi-jointed, the angular flapping rate may be different across different sections of the same semispan, and because the bones and wingtip feathers of a bird's wing are not rigid, the angular rate could vary continuously across each wing semispan.[5]

In addition to the wing planform shape $c(z)$, the lifting-line solution in Eqs. (10)–(26) depends on five separate time-dependent functions that describe the details of the flapping cycle, i.e., $\omega(z,t)$, $\psi(z,t)$, $C_L(t)$, $\Omega(t)$, and $\hat{p}(t)$. Any or all of these five time-dependent functions could be varied to improve or optimize some measure of flight performance.

One advantage of the lifting-line solution presented in Eqs. (10)–(26) is that it allows us to decompose and examine separately the contributing factors associated with the lift, drag, and power coefficients, even when the wing flapping motion is very complex. However, to gain insight into the three-dimensional production of induced thrust along the span of a flapping wing it is convenient to commence with simple motion and progress to the more complex. Here we start by considering simple **rigid-semispan flapping of an untwisted wing in pure plunging**.

Because wing flapping is periodic, the mean value of the flapping rate averaged over a complete flapping cycle is always zero. Hence, **if the decomposed Fourier coefficients, root aerodynamic angle of attack, and washout remain fixed over the flapping cycle**, the mean lift coefficient is found from Eq. (13) to be

$$\overline{C}_L = \pi R_A[a_1(\alpha - \alpha_{L0})_{\text{root}} - b_1\Omega] \tag{27}$$

and the instantaneous lift coefficient given by Eq. (13) can be written equivalently as

$$C_L = \overline{C}_L + \pi R_A d_1 \hat{p} \tag{28}$$

where the decomposed Fourier coefficient d_1 is obtained from Eq. (12). This instantaneous lift coefficient is greater than the mean value during the downstroke when $\hat{p}$ is defined to be positive, and it is less than the mean during the upstroke when $\hat{p}$ is negative. This type of wing flapping is referred to as pure plunging, because the airfoil sections of the wing are not rotating in pitch during the flapping cycle. Using Eqs. (15) and (28) in Eqs. (14) and (23) for the case of an **untwisted wing** yields

$$C_{D_i} = \frac{(1+\kappa_D)}{\pi R_A}\overline{C}_L^2 - \frac{\kappa_{Lp} - 2(1+\kappa_D)(d_1/a_1)}{\pi R_A}\overline{C}_L C_{L,\alpha}\hat{p} - \frac{\kappa_p + \kappa_{Lp}(d_1/a_1) - (1+\kappa_D)(d_1/a_1)^2}{\pi R_A}(C_{L,\alpha}\hat{p})^2 \tag{29}$$

$$C_{P_f} = 4[\kappa_a\overline{C}_L + (\kappa_d + \kappa_a\, d_1/a_1)C_{L,\alpha}\hat{p}]\hat{p} \tag{30}$$

To obtain numerical results from Eqs. (29) and (30), the plunging distribution function $\psi(\theta)$ must be known. If the semispans are rigid, there can be no bending of either semispan, and the angular rate is constant across each semispan. As shown schematically in Fig. 2, if the flapping rate is spanwise symmetric about the midspan, the plunging distribution function ψ for **small-angle flapping with no semispan bending** is given by[5]

$$\psi(z) = \begin{cases} -2z/b, & z<0 \\ 2z/b, & z>0 \end{cases} \quad \text{or} \quad \psi(\theta) = \left|\cos(\theta)\right| \tag{31}$$

Using Eq. (31) in Eq. (22) yields a closed-form relation for the coefficients e_n for the special case of **small-angle flapping with no semispan bending**,[5] i.e.,

$$e_n \equiv \begin{cases} \dfrac{(-1)^{(n+1)/2}\,4}{(n^2-4)\pi}, & \text{for } n \text{ odd} \\ 0, & \text{for } n \text{ even} \end{cases} \tag{32}$$

The plunging distribution function given in Eq. (31) is based on defining the magnitude of the flapping rate, p, to be positive when the wingtips are moving downward relative to the wing root. To account for the wing joints and elastic deformation of some particular bird's wing, a more complex function would be required for ψ.

Because the mean value of $\hat{p}$ is zero for periodic flapping, from Eqs. (29) and (30) the mean induced-drag and flapping-power coefficients for **flapping of an untwisted wing in pure plunging** are

$$\overline{C}_{D_i} = \frac{(1+\kappa_D)}{\pi R_A}\overline{C}_L^2 - \frac{\kappa_p + \kappa_{Lp}(d_1/a_1) - (1+\kappa_D)(d_1/a_1)^2}{\pi R_A}(C_{L,\alpha}\hat{p}_{\text{rms}})^2 \tag{33}$$

$$\overline{C}_{P_f} = 4(\kappa_d + \kappa_a\, d_1/a_1)C_{L,\alpha}\hat{p}_{\text{rms}}^2 \tag{34}$$

where $\hat{p}_{\text{rms}}$ is the root mean square (rms) dimensionless flapping rate. The first term on the right-hand side of Eq. (33) is the induced drag for the same wing geometry with no wing flapping. The aerodynamic force associated

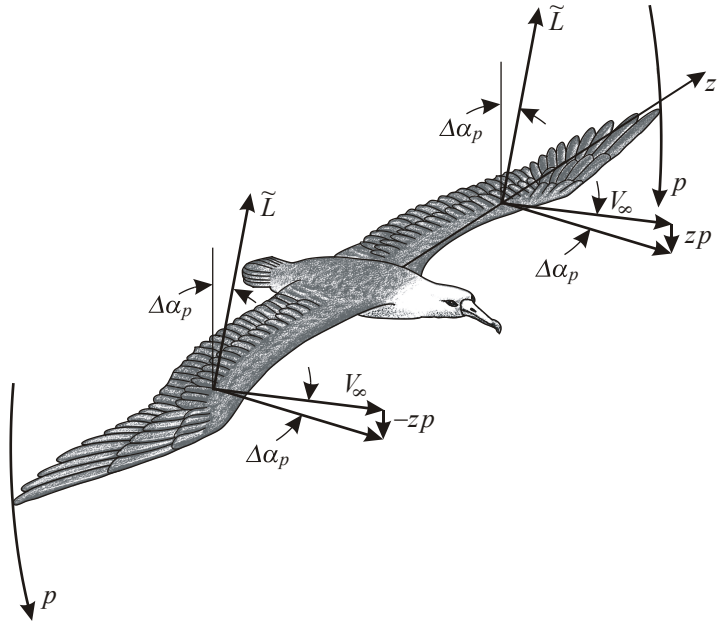

Figure 2. Change in the local section geometric angle of attack on a bird's wing resulting from the plunging motion associated with wing flapping.

with the second term on the right-hand side of Eq. (33) is always aligned with the direction of flight. This is the ***mean induced thrust***, which is developed by the **flapping of an untwisted wing in pure plunging**,[5] i.e.,

$$\overline{T}_f = \tfrac{1}{2}\rho V_\infty^2 S \frac{\kappa_p + \kappa_{Lp}(d_1/a_1) - (1+\kappa_D)(d_1/a_1)^2}{\pi R_A}(C_{L,\alpha}\hat{p}_{\rm rms})^2 \tag{35}$$

The mean available propulsive power developed by this wing flapping is simply the product of the mean induced thrust and the airspeed.[5] Hence, from Eq. (35), the ***mean available-power coefficient*** for **flapping of an untwisted wing in pure plunging** is

$$\overline{C}_{P_A} \equiv \frac{\overline{T}_f V_\infty}{\tfrac{1}{2}\rho V_\infty^3 S} = \frac{\kappa_p + \kappa_{Lp}(d_1/a_1) - (1+\kappa_D)(d_1/a_1)^2}{\pi R_A}(C_{L,\alpha}\hat{p}_{\rm rms})^2 \tag{36}$$

The ***ideal propulsive efficiency***[5] for **flapping of an untwisted wing in pure plunging** is the mean available-power coefficient from Eq. (36) divided by the required mean flapping-power coefficient from Eq. (34), i.e.,

$$\eta_p \equiv \frac{\overline{C}_{P_A}}{\overline{C}_{P_f}} = \frac{\kappa_p a_1^2 + \kappa_{Lp} a_1 d_1 - (1+\kappa_D) d_1^2}{4(\kappa_d a_1 + \kappa_a d_1)} \tag{37}$$

To maintain steady periodic motion, the mean induced thrust obtained from the second term on the right-hand side of Eq. (33) must balance the induced-drag component that is obtained from the first term on the right-hand side of Eq. (33) combined with the mean parasitic drag. Thus, from Eq. (33), **steady periodic flapping of an untwisted wing in pure plunging** with a constant parasitic-drag coefficient of C_{D_p} requires

$$\hat{p}_{\rm rms} = \frac{1}{C_{L,\alpha}} \sqrt{\frac{\pi R_A}{\kappa_p + \kappa_{Lp}(d_1/a_1) - (1+\kappa_D)(d_1/a_1)^2} \left[C_{D_p} + \frac{(1+\kappa_D)}{\pi R_A}\overline{C}_L^2 \right]} \tag{38}$$

To maintain constant altitude the mean lift must support the weight, i.e.,

$$\overline{C}_L = \frac{W}{\tfrac{1}{2}\rho V_\infty^2 S} \tag{39}$$

and the total drag for this **untwisted wing in the absence of wing flapping** can be written as

$$D = \tfrac{1}{2}\rho V_\infty^2 S \left[C_{D_p} + \frac{(1+\kappa_D)}{\pi R_A}\overline{C}_L^2 \right] = W \left[\frac{C_{D_p}}{\overline{C}_L} + \frac{(1+\kappa_D)}{\pi R_A}\overline{C}_L \right] \tag{40}$$

Hence, **constant-altitude flight of an untwisted wing at a forward speed equal to the minimum-drag airspeed without flapping** requires

$$\overline{C}_L = \sqrt{\frac{\pi R_A C_{D_p}}{1+\kappa_D}} \tag{41}$$

Wing-flapping cycles are often assumed to be sinusoidal. With this arbitrary assumption, the instantaneous dimensionless flapping rate is easily related to the rms dimensionless flapping rate to give

$$\hat{p} = \sqrt{2}\,\hat{p}_{\rm rms} \sin(2\pi t/\tau) \tag{42}$$

Applying Eqs. (38) and (42) to Eqs. (28)–(30) yields the instantaneous lift, induced-drag, and flapping-power coefficients for **steady sinusoidal flapping of an untwisted wing in pure plunging**. For example, the lift coefficient is

$$C_L = \overline{C}_L + \frac{\pi R_A d_1}{C_{L,\alpha}} \sqrt{\frac{2\pi R_A}{\kappa_p + \kappa_{Lp}(d_1/a_1) - (1+\kappa_D)(d_1/a_1)^2} \left[C_{D_p} + \frac{(1+\kappa_D)}{\pi R_A} \overline{C}_L^2 \right]} \sin(2\pi t/\tau) \tag{43}$$

As an example of steady sinusoidal flapping in pure plunging, consider an untwisted rectangular wing of aspect ratio 14 with an airfoil section lift slope of 2π. Using $b/c = 14.0$, $\widetilde{C}_{L,\alpha} = 2\pi$, and $\psi(\theta)$ specified by Eq. (31), the decomposed Fourier coefficients, a_n, d_n, and e_n, are obtained from Eqs. (10), (12), and (32), respectively. Applying the results to Eqs. (15), (16), (19), (21), (24), and (26), yields

$$C_{L,\alpha} = 5.3154, \qquad \kappa_D = 0.1191, \qquad \kappa_{Lp} = 3.6067, \qquad \kappa_p = 0.3357, \qquad \kappa_a = 0.1171, \qquad \kappa_d = 0.01545$$

For these computations, we assume a reasonable parasitic-drag coefficient of 0.01 and a flight speed equal to the minimum-drag airspeed without flapping. To maintain airspeed and altitude with sinusoidal flapping, Eq. (38) requires $\hat{p}_{\text{rms}} = 0.1323$, and Eqs. (41)–(43) yield

$$\hat{p} = 0.1871 \sin(2\pi t/\tau)$$

$$C_L = 0.6269 + 0.4656 \sin(2\pi t/\tau)$$

Results obtained from Eqs. (28)–(30) for this untwisted rectangular wing are shown in Fig. 3. The ideal propulsive efficiency obtained from Eq. (37) for this flapping cycle is 76.5%.

From the definition of $\hat{p}$ combined with Eqs. (39) and (42), the sinusoidal flapping rate can be written as

$$p = \frac{\sqrt{8}\hat{p}_{\text{rms}} V_\infty}{b} \sin(2\pi t/\tau) = \frac{4\hat{p}_{\text{rms}}}{b} \sqrt{\frac{W}{\rho S \overline{C}_L}} \sin(2\pi t/\tau) \tag{44}$$

This same sinusoidal flapping motion can be defined by expressing the instantaneous flapping dihedral angle, ϕ, in terms of its sinusoidal amplitude, ϕ_A, i.e.,

$$\phi = \phi_A \cos(2\pi t/\tau) \tag{45}$$

Because p is the angular rate at which the dihedral angle is decreasing, from Eq. (45) we obtain

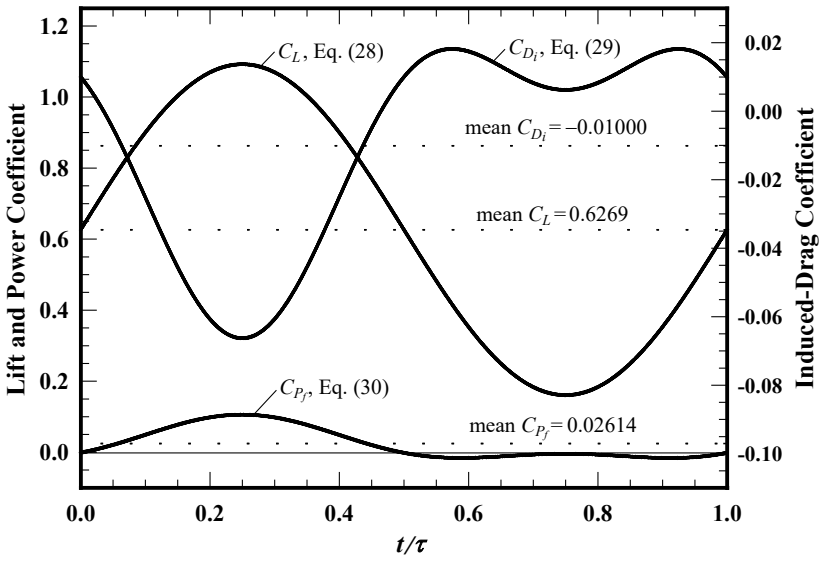

Figure 3. Variations in lift, induced-drag, and flapping-power coefficients as predicted by Eqs. (28)–(30) for sinusoidal flapping of an untwisted rectangular wing of aspect ratio 14.

$$p \equiv -\frac{d\phi}{dt} = \frac{2\pi\phi_A}{\tau}\sin(2\pi t/\tau) \tag{46}$$

Combining Eqs. (44) and (46), the flapping period required to maintain airspeed at constant altitude with sinusoidal flapping can be written as

$$\tau = \frac{\pi\phi_A}{2\hat{p}_{\text{rms}}}\sqrt{\overline{C_L}}\,\frac{b}{\sqrt{W/(\rho S)}} \tag{47}$$

Using the wing planform area and weight of a large golden eagle, with an assumed sinusoidal flapping amplitude of $\pm 15°$ ($15\pi/180$), a 6-ft^2 wing area, and a weight of 9 lbf, the flapping cycle shown in Fig. 3 requires a flapping period at standard sea level of 0.90 s and an airspeed of 45 ft/s. This rectangular wing has a chord length of 0.65 ft, so the product of the chord length and the flapping frequency divided by the airspeed is about 0.10, which is consistent with the quasi-steady solution.[6]

II. Optimizing Wing Twist for Maximum Propulsive Efficiency

To gain insight into the effects of wing twist on the performance of a flapping wing in forward flight, we shall now relax the assumptions of no twist and pure plunging. However, to isolate the effects of wing twist, we will retain the assumptions of sinusoidal flapping and no bending of the wing semispans. Hence, we shall continue to use the time-independent plunging distribution function $\psi(z)$ that is given by Eq. (31). In addition, we will continue to use the sinusoidal flapping rate $\hat{p}(t)$ as given by Eq. (42), and we will maintain a sinusoidal variation in the wing lift coefficient $C_L(t)$, which is in phase with the flapping rate, i.e.,

$$C_L = \overline{C_L} + C_{LA}\sin(2\pi t/\tau) \tag{48}$$

To maintain this sinusoidal variation in wing lift coefficient for arbitrary variations in the washout functions $\omega(z,t)$ and $\Omega(t)$, Eqs. (13) and (15) require that the root aerodynamic angle of attack must be varied over the flapping cycle to maintain the relation

$$(\alpha - \alpha_{L0})_{\text{root}} = \frac{C_L}{C_{L,\alpha}} + \frac{b_1}{a_1}\Omega - \frac{d_1}{a_1}\hat{p} \tag{49}$$

A bird or ornithopter could accomplish this in flight by rotating the wing semispans and/or coordinating a periodic motion of the tail with that of the wing.

The instantaneous induced-drag coefficient predicted by lifting-line theory during small-angle wing flapping can be evaluated from Eq. (14), and the instantaneous flapping-power coefficient required to support small-angle flapping of spanwise symmetric wings is obtained from Eq. (23). Hence, when the induced drag produced by wing flapping is negative, the instantaneous power input per unit induced thrust could be minimized by minimizing the negative dimensionless ratio that is given by

$$\frac{C_{D_i}}{C_{P_f}} = \frac{(1+\kappa_D)C_L^2 - \kappa_{Lp}C_L C_{L,\alpha}\hat{p} - \kappa_p(C_{L,\alpha}\hat{p})^2 + \kappa_{D\Omega}(C_{L,\alpha}\Omega)^2 - (\kappa_{DL}C_L - \kappa_{\Omega p}C_{L,\alpha}\hat{p})C_{L,\alpha}\Omega}{4\pi R_A(\kappa_a C_L - \kappa_b C_{L,\alpha}\Omega + \kappa_d C_{L,\alpha}\hat{p})\hat{p}} \tag{50}$$

For example, the instantaneous washout magnitude $\Omega(t)$ that requires minimum power input per unit induced thrust for any given values of $\omega(z,t)$, $\psi(z,t)$, $C_L(t)$, and $\hat{p}(t)$ can be obtained by differentiating the ratio defined in Eq. (50) with respect to Ω, setting the result to zero, and solving for Ω. However, $\hat{p}$ is always zero at two instants during a flapping cycle, and the denominator on the right-hand side of Eq. (50) is always zero when $\hat{p}$ is zero, independent of $\omega(z,t)$, $\Omega(t)$, $\psi(z,t)$, and $C_L(t)$. This is not a problem for the optimization with respect to $\Omega(t)$, because this optimization can be carried out analytically. On the other hand, for numerical optimization with respect to $\omega(z,t)$, it is more convenient to define a slightly different dimensionless optimization ratio.

For the purpose of either analytical or numerical optimization of wing twist, when computing derivatives of the right-hand side of Eq. (50) with respect to the wing twist parameters, $\hat{p}$ and C_L are held constant. Hence, the instantaneous power input per unit induced thrust can be minimized equivalently by minimizing the dimensionless ratio that is defined by multiplying Eq. (50) through by $4\pi R_A\hat{p}/C_L$, i.e.,

$$R_O \equiv \frac{1+\kappa_D-\kappa_{Lp}\dfrac{C_{L,\alpha}\hat{p}}{C_L}-\kappa_p\left(\dfrac{C_{L,\alpha}\hat{p}}{C_L}\right)^2+\kappa_{D\Omega}\left(\dfrac{C_{L,\alpha}\Omega}{C_L}\right)^2-\left(\kappa_{DL}-\kappa_{\Omega p}\dfrac{C_{L,\alpha}\hat{p}}{C_L}\right)\dfrac{C_{L,\alpha}\Omega}{C_L}}{\kappa_a-\kappa_b\dfrac{C_{L,\alpha}\Omega}{C_L}+\kappa_d\dfrac{C_{L,\alpha}\hat{p}}{C_L}} \tag{51}$$

The instantaneous washout magnitude $\Omega(t)$ that requires minimum power input per unit induced thrust for any given values of $\omega(z,t)$, $\psi(z,t)$, $C_L(t)$, and $\hat{p}(t)$ could be obtained by differentiating either the ratio defined in Eq. (50) or that defined in Eq. (51) with respect to Ω, setting the result to zero, and solving for Ω. However, notice that in addition to the wing coefficients defined in Eqs. (15)–(21) and (24)–(26), the ratio that is defined in Eq. (50) depends on three time-dependent operating parameters, $\Omega(t)$, $C_L(t)$, and $\hat{p}(t)$. On the other hand, the ratio defined in Eq. (51) depends on only the wing coefficients and two operating parameters, $C_{L,\alpha}\Omega/C_L$ and $C_{L,\alpha}\hat{p}/C_L$. Hence, from the ratio defined in Eq. (51), the instantaneous operating parameter $C_{L,\alpha}\Omega/C_L$ that requires **minimum power input per unit induced thrust** for any given values of $\omega(z,t)$, $\psi(z,t)$, and $C_{L,\alpha}\hat{p}/C_L$ can be obtained from

$$\frac{C_{L,\alpha}\Omega_{\text{opt}}}{C_L} = \frac{\kappa_a}{\kappa_b}+\frac{\kappa_d}{\kappa_b}\frac{C_{L,\alpha}\hat{p}}{C_L}\pm\sqrt{C_0+C_1\frac{C_{L,\alpha}\hat{p}}{C_L}+C_2\left(\frac{C_{L,\alpha}\hat{p}}{C_L}\right)^2} \tag{52}$$

where

$$C_0 \equiv \frac{1+\kappa_D}{\kappa_{D\Omega}}+\frac{\kappa_a^2}{\kappa_b^2}-\frac{\kappa_a\kappa_{DL}}{\kappa_b\kappa_{D\Omega}} \tag{53}$$

$$C_1 \equiv \frac{\kappa_a\kappa_{\Omega p}}{\kappa_b\kappa_{D\Omega}}+2\frac{\kappa_a\kappa_d}{\kappa_b^2}-\frac{\kappa_{Lp}}{\kappa_{D\Omega}}-\frac{\kappa_d\kappa_{DL}}{\kappa_b\kappa_{D\Omega}} \tag{54}$$

$$C_2 \equiv \frac{\kappa_d\kappa_{\Omega p}}{\kappa_b\kappa_{D\Omega}}+\frac{\kappa_d^2}{\kappa_b^2}-\frac{\kappa_p}{\kappa_{D\Omega}} \tag{55}$$

Depending on $c(z)$, $\omega(z,t)$, $\psi(z,t)$, $C_L(t)$, and $\hat{p}(t)$, either of the two roots obtained from Eq. (52) could be the one of interest, which produces net mean thrust and minimizes the required power input per unit induced thrust. The root that is not of interest for this purpose may correspond to a power generation mode, which yields negative power input and positive induced drag. Because thrust generation yields negative induced drag and positive power input, both roots could result in negative values of the ratio defined in Eq. (50). Furthermore, the power generation mode can result in a negative value of this ratio that is less than that associated with the thrust generation mode. Hence, the sign preceding the square root in Eq. (52) must be chosen carefully.

For the case of wing flapping with **linear washout and no semispan bending**, both the washout distribution function ω and the plunging distribution function ψ are time independent and equal[5]

$$\omega(z) = \psi(z) = \begin{cases} -2z/b, & z<0 \\ 2z/b, & z>0 \end{cases} \quad \text{or} \quad \omega(\theta) = \psi(\theta) = \left|\cos(\theta)\right| \tag{56}$$

Applying Eq. (56) to Eqs. (11) and (12) yields

$$b_n = d_n \tag{57}$$

and using Eqs. (57), (17)–(21), and (24)–(26) in Eqs. (54) and (55) results in

$$C_1 = C_2 = 0 \tag{58}$$

Hence, after applying Eqs. (53), (57), and (58) to Eq. (52), we find that for the special case of wing flapping with **linear washout and no semispan bending**, the instantaneous amount of wing washout $C_{L,\alpha}\Omega/C_L$ that requires **minimum power input per unit induced thrust** for any given value of $C_{L,\alpha}\hat{p}/C_L$ can be obtained from

$$\frac{C_{L,\alpha}\Omega_{\text{opt}}}{C_L} = \frac{\kappa_a}{\kappa_b} \pm \sqrt{\frac{1+\kappa_D}{\kappa_{D\Omega}} + \frac{\kappa_a^2}{\kappa_b^2} - \frac{\kappa_a \kappa_{DL}}{\kappa_b \kappa_{D\Omega}}} + \frac{C_{L,\alpha}\hat{p}}{C_L} \tag{59}$$

If both the lift coefficient and the flapping rate are sinusoidal and in phase, $\hat{p}(t)$ and $C_L(t)$ can be obtained from Eqs. (42) and (48), respectively. Using these relations and Eq. (52) in Eq. (14), with the **minimum-power washout magnitude maintained over the flapping cycle**, the instantaneous induced-drag coefficient can be computed at each instant in the flapping cycle for any given values of $\omega(z,t)$, $\psi(z,t)$, $\overline{C}_L$, C_{LA}, and $\hat{p}_{\text{rms}}$. The mean induced-drag coefficient is computed from numerical integration of the results obtained from Eq. (14), and $\hat{p}_{\text{rms}}$ is obtained by numerically finding the value that gives $\overline{C}_{D_i} = -C_{D_p}$. The mean flapping-power coefficient is then computed from numerical integration of the results obtained from Eq. (23).

Using the time-independent linear washout and plunging distribution functions ω and ψ as specified by Eq. (56) combined with the same wing planform and sinusoidal lift coefficient that were used to obtain the results shown in Fig. 3 produces

$$C_0 = 52.209, \qquad C_1 = 0.0, \qquad C_2 = 0.0,$$

$$\frac{C_{L,\alpha}\Omega_{\text{opt}}}{C_L} = 0.3487 + \frac{C_{L,\alpha}\hat{p}}{C_L}$$

and the results shown in Fig. 4. Notice that by maintaining the minimum-power washout magnitude at each instant during the flapping cycle, we have reduced the required mean flapping-power coefficient from 0.02614 to 0.02194. This reduction in required power results from a substantial reduction in torque with only a slight reduction in induced thrust for a given value of $\hat{p}_{\text{rms}}$. To maintain airspeed and altitude with sinusoidal flapping, the rms flapping rate is increased slightly from $\hat{p}_{\text{rms}} = 0.1323$ to $\hat{p}_{\text{rms}} = 0.1492$, which reduces the flapping period at standard sea level from 0.90 s to 0.80 s. The net result is an increase in the ideal propulsive efficiency for this flapping cycle from 76.5% to 91.2%.

The periodic motion associated with the flapping cycle shown in Fig. 3 is pure plunging, i.e., the airfoil sections of the wing are not rotating in pitch during the flapping cycle. On the other hand, the flapping cycle shown in Fig. 4 is composed of a combination of periodic plunging and pitching motion. As the airfoil sections of this wing plunge and heave periodically at a rate that depends on both the spanwise coordinate and time, these sections are also rotating in pitch at a rate that varies with z and t. The instantaneous angle that the zero-lift line for each airfoil

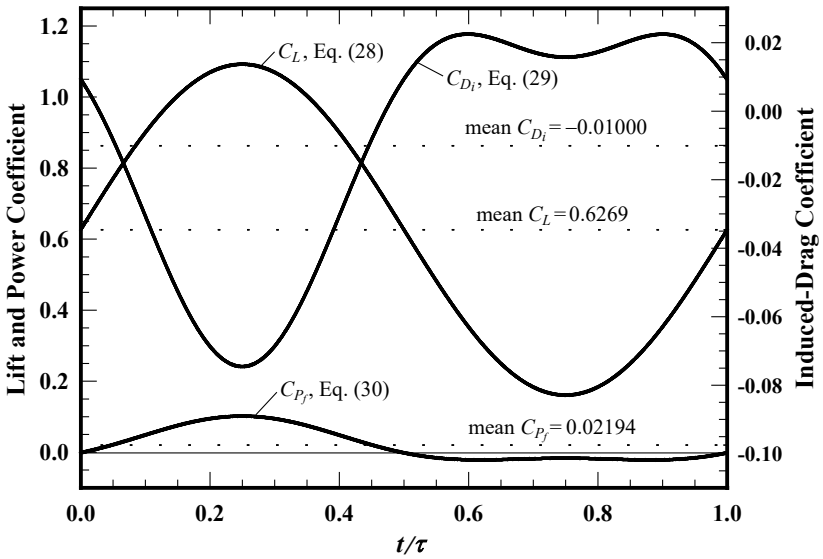

Figure 4. Lift, induced-drag, and flapping-power coefficients for a rectangular wing of aspect ratio 14 with sinusoidal flapping, linear washout, and the minimum-power washout magnitude.

section makes with the freestream is the local aerodynamic angle of attack, which is the root aerodynamic angle of attack less the product of the washout distribution function and the washout magnitude, i.e., $(\alpha - \alpha_{L0})_{\text{root}} - \omega\Omega$. For the wing flapping cycle shown in Fig. 4, the root aerodynamic angle of attack is specified by Eq. (49), the washout distribution function is given by Eq. (56), and the washout magnitude is obtained from Eq. (59).

The easiest way to visualize the combined plunging–pitching motion associated with the flapping cycle shown in Fig. 4 is from slow-motion video. However, some insight into this complex motion can be gained by examining the plunging and pitching separately. The section plunging motion can be described simply in terms of the variation with time t of the y coordinate of the airfoil-section aerodynamic center located at the spanwise coordinate z. Within the small angle approximation, this section plunging varies linearly with z and is sinusoidal in t, i.e.,

$$y_{ac}(z,t) = |z|\,\phi_A \cos(2\pi t/\tau) \tag{60}$$

For small dihedral amplitudes, the local angle of attack increment that results from this plunging motion is also approximated as a linear function of z and a sinusoidal function of t, i.e.,

$$\Delta\alpha_p(z,t) = \sqrt{8}\,\hat{p}_{\text{rms}}\,|z/b|\sin(2\pi t/\tau) \tag{61}$$

This is the angle between the freestream and the instantaneous local relative wind, at the spanwise coordinate z and time t. The variation in this plunging angle of attack increment with z and t is shown in Fig. 5.

The section pitching motion that is superimposed on this plunging motion depends on z and t as shown in Fig. 6. The curve in the right-hand view of this figure, which is labeled "wing root" and corresponds to z/b=0.00, shows how the root aerodynamic angle of attack specified by Eq. (49) varies with time. The difference between this root aerodynamic angle of attack and that for any other wing section is the local section twist, which is shown in Fig. 7. Notice in Fig. 6 that the local aerodynamic angle of attack is less than that for the root over the entire downstroke. Because washout is defined traditionally to be positive twist, the instantaneous wing twist shown in Fig. 7 is positive whenever the local aerodynamic angle of attack is less than that for the root. Therefore, we see from both Fig. 6 and Fig. 7 that the washout is positive over the entire downstroke and negative over much of the upstroke. The wingtip curve in the right-hand view of Fig. 7 that corresponds to z/b=0.50 is the washout magnitude $\Omega(t)$ obtained from Eq. (59).

The relative section angle of attack shown in Fig. 8 is defined here to be the instantaneous angle that the zero-lift line for each airfoil section makes with the local section relative wind. This is an effective aerodynamic angle of attack for each airfoil section, which is obtained simply by adding the plunging angle of attack increment that is shown in Fig. 5 to the freestream aerodynamic angle of attack that is shown in Fig. 6. Notice from the results shown in Fig. 8 that this effective aerodynamic angle of attack is always greatest at the wing root and decreases linearly from the root to the wingtip.

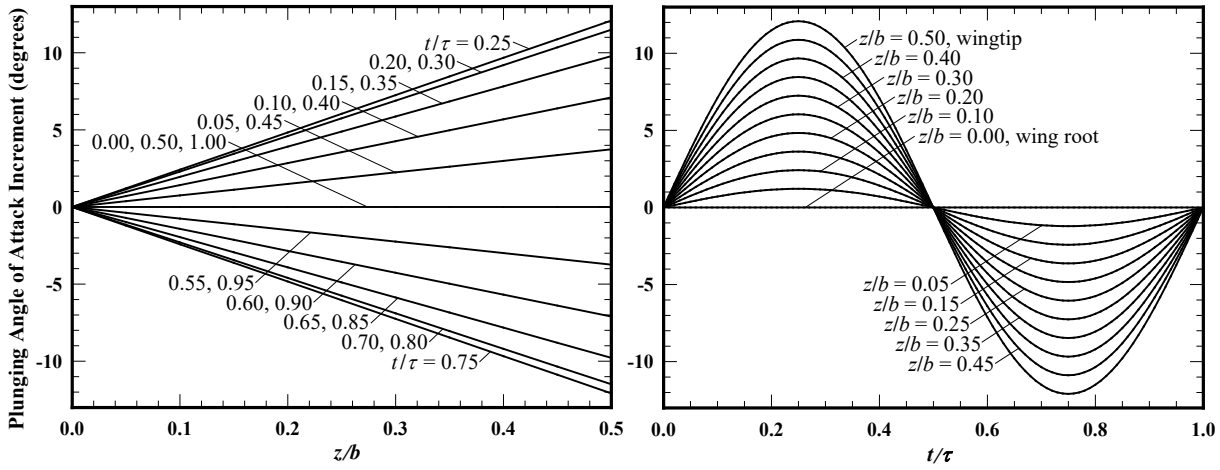

Figure 5. Plunging angle of attack increment for a rectangular wing of aspect ratio 14 with sinusoidal flapping, linear washout, and the minimum-power washout magnitude.

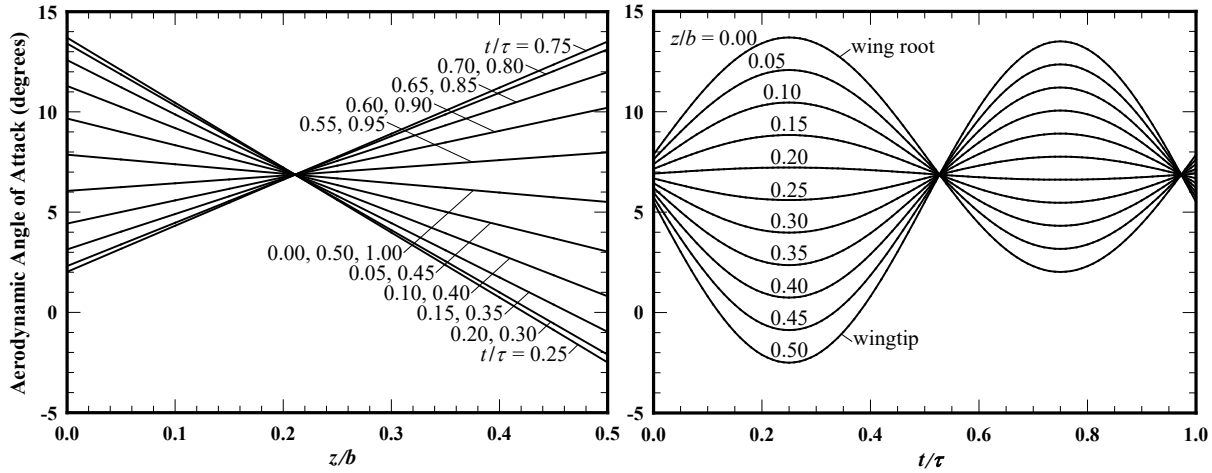

Figure 6. Pitching motion for a rectangular wing of aspect ratio 14 with sinusoidal flapping, linear washout, and the minimum-power washout magnitude.

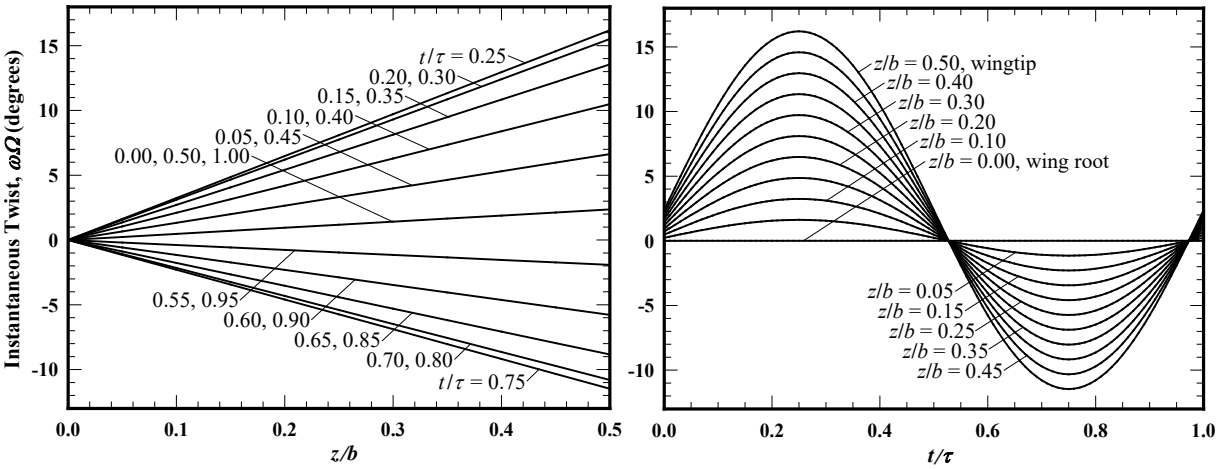

Figure 7. Instantaneous wing twist for a rectangular wing of aspect ratio 14 with sinusoidal flapping, linear washout, and the minimum-power washout magnitude.

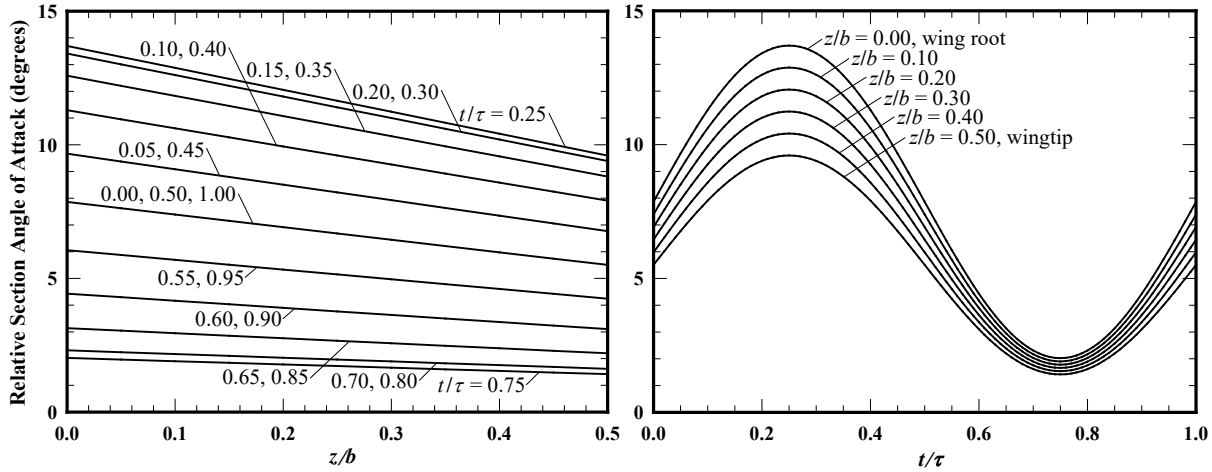

Figure 8. Relative section angle of attack for a rectangular wing of aspect ratio 14 with sinusoidal flapping, linear washout, and the minimum-power washout magnitude.

If the washout magnitude $\Omega(t)$ is varied over the flapping cycle such that Eq. (52) is always satisfied using the appropriate root, the resulting flapping cycle will produce maximum possible propulsive efficiency for any arbitrary set of the functions $c(z)$, $\omega(z,t)$, $\psi(z,t)$, $C_L(t)$, and $\hat{p}(t)$. However, it should be noted that **this maximum is not necessarily a global maximum** unless the functions $\omega(z,t)$, $\psi(z,t)$, $C_L(t)$, and $\hat{p}(t)$ are also optimized for maximum propulsive efficiency. For example, it is possible to improve the propulsive efficiency over that obtained for the flapping cycle shown in Figs. 4–8 by optimizing the product $\omega(z,t)\Omega(t)$ to minimize the ratio defined in Eq. (51).

To demonstrate how the product $\omega(z,t)\Omega(t)$ can be optimized for minimum required power per unit induced thrust, a variable twist distribution was defined using M control points spaced along the span of the wing. With M always chosen to be odd, one control point was placed at each wingtip, another at the midspan, and the intermediate control points were spaced uniformly in θ. The control-point values used for the twist distribution $\omega(z,t)\Omega(t)$ were constrained to be spanwise symmetric and 0.0 at the midspan. The $(M-1)/2$ unknown values of $\omega(z,t)\Omega(t)$ at the remaining control points were treated as independent scalar variables, to be evaluated from numerical optimization. The values used for the $\omega(z,t)\Omega(t)$ product between control points were evaluated using linear interpolation in θ. At each instant in time during the flapping cycle, the $(M-1)/2$ unknown control-point values of the $\omega(z,t)\Omega(t)$ product were found using a computer optimization algorithm.[11,12] This optimization software minimizes a single fitness parameter, which in this case was chosen to be the ratio defined in Eq. (51). The optimization software used to find the control-point values of the $\omega(z,t)\Omega(t)$ product implements the BFGS algorithm, named after the work of Broyden,[13] Fletcher,[14] Goldfarb,[15] and Shanno.[16]

To assure that the numerical solutions were grid resolved, independent solutions were obtained using coarse and fine grids. The coarse-grid solutions used $M=19$ and $N=39$. For the fine-grid solutions $M=39$ and $N=199$ were used. Over the range of parameters studied, the coarse-grid solutions for propulsive efficiency were found to agree with the fine-grid solutions to within 0.03%. For the temporal variations, both 50 and 100 time steps per cycle were used with second-order trapezoidal numerical integration. Over the range of parameters studied, the 50 time-step solutions for propulsive efficiency were found to agree with the 100 time-step solutions to within 5×10^{-10}%.

Using this numerical optimization with sinusoidal flapping and the plunging distribution function $\psi(z)$ for no semispan bending given by Eq. (31), combined with the same wing planform and sinusoidal lift coefficient that were used to obtain the results shown in Figs. 3 and 4, produces the results shown in Figs. 9–13. Comparing the flapping cycle shown in Fig. 4 with that shown in Fig. 9, we find that by maintaining the minimum-power twist distribution–magnitude product $\omega(z,t)\Omega(t)$ at each instant during the flapping cycle, we have gained a small additional reduction in the required mean flapping-power coefficient from 0.02194 to 0.02174. To maintain airspeed and altitude with sinusoidal flapping, the rms flapping rate is decreased slightly from $\hat{p}_{\text{rms}}=0.1492$ to $\hat{p}_{\text{rms}}=0.1467$. The net result is a slight increase in the ideal propulsive efficiency for this flapping cycle from 91.2% to 92.0%.

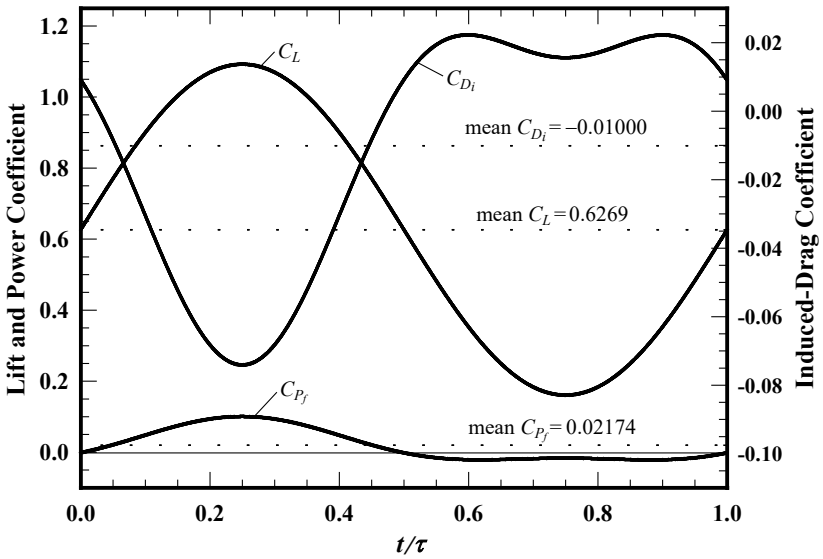

Figure 9. Lift, induced-drag, and flapping-power coefficients for a rectangular wing of aspect ratio 14 with sinusoidal flapping and the minimum-power twist distribution–magnitude product.

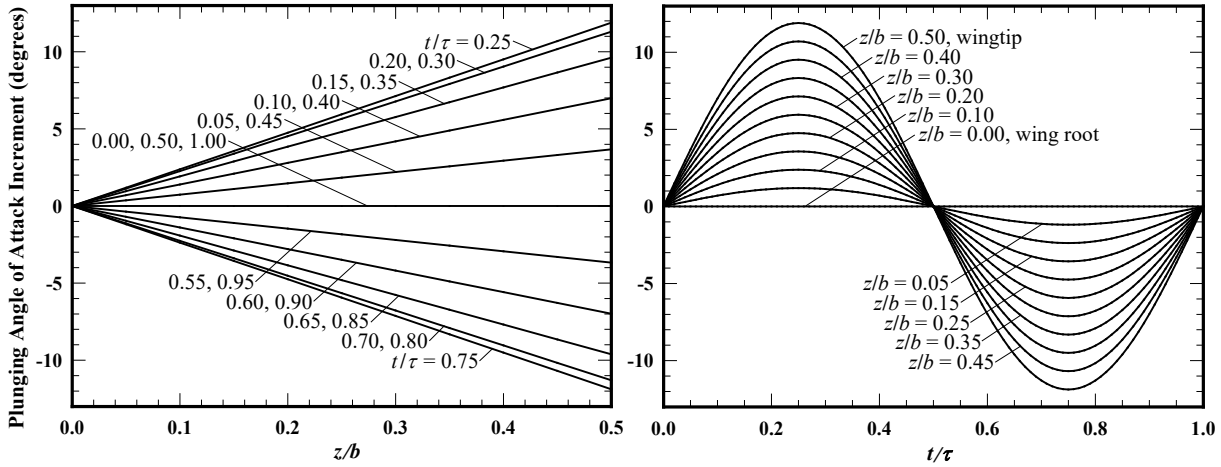

Figure 10. Plunging angle of attack increment for a rectangular wing of aspect ratio 14 with sinusoidal flapping and the minimum-power twist distribution–magnitude product.

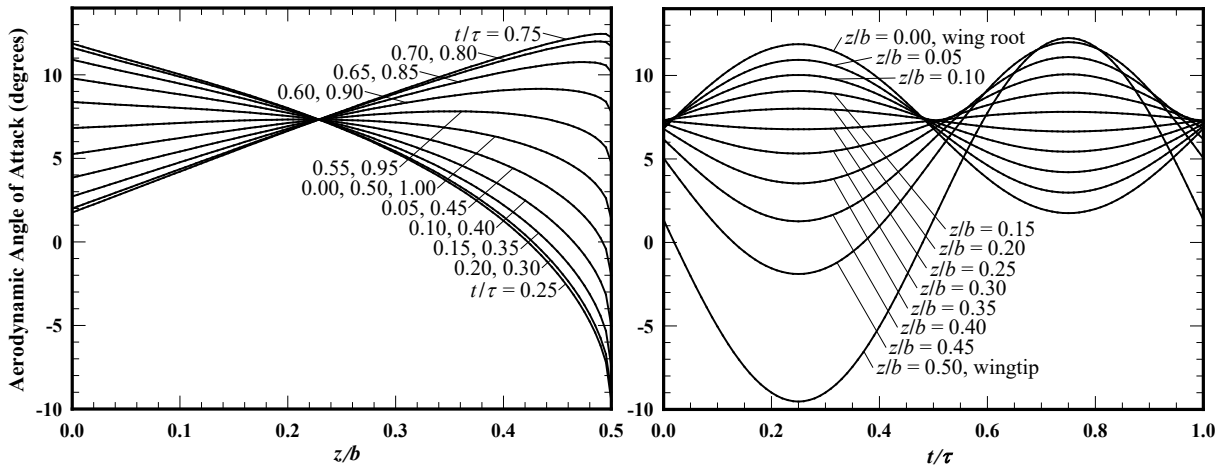

Figure 11. Pitching motion for a rectangular wing of aspect ratio 14 with sinusoidal flapping and the minimum-power twist distribution–magnitude product.

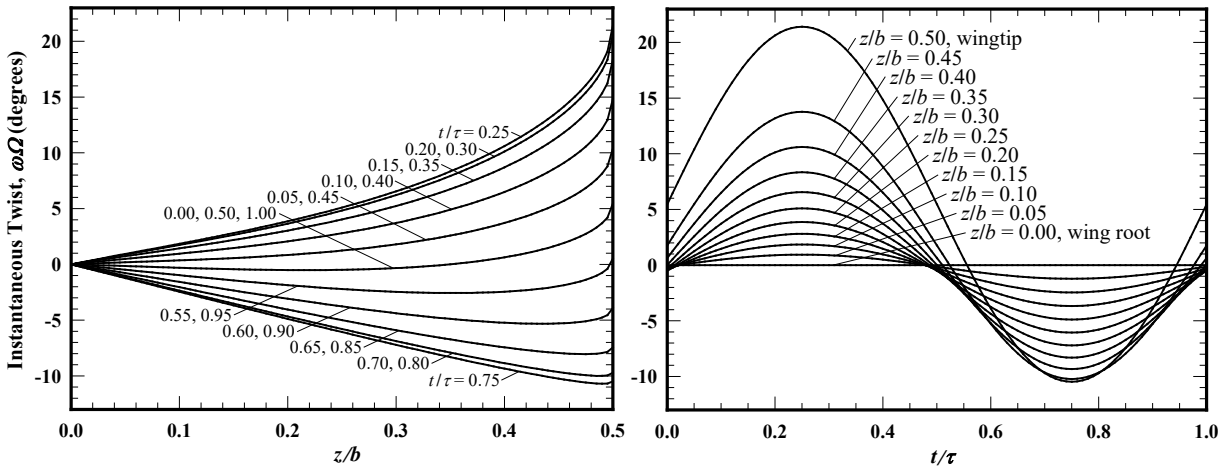

Figure 12. Instantaneous wing twist for a rectangular wing of aspect ratio 14 with sinusoidal flapping and the minimum-power twist distribution–magnitude product.

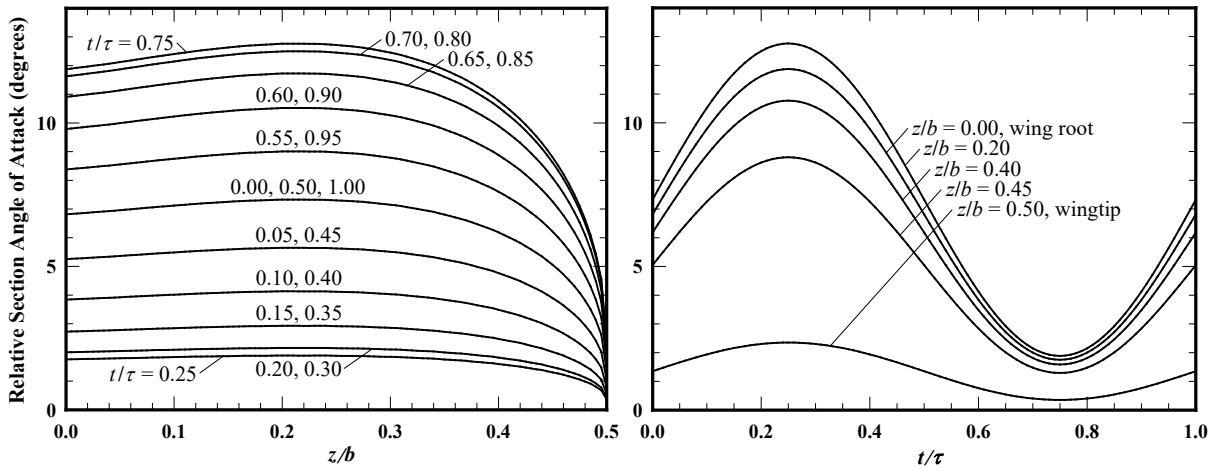

Figure 13. Relative section angle of attack for a rectangular wing of aspect ratio 14 with sinusoidal flapping and the minimum-power twist distribution–magnitude product.

For the results shown in Fig. 4, the time-independent linear washout distribution function specified by Eq. (56) was used with the minimum-power washout magnitude obtained from Eq. (52). The results shown in Fig. 9 were obtained using the time-varying minimum-power twist distribution–magnitude product $\omega(z,t)\Omega(t)$, which is shown in Fig. 12. As was the case for the flapping cycle used to obtain the results shown in Fig. 4, the small-angle section plunging motion with no semispan bending as described by Eqs. (60) and (61) was used to obtain the results shown in Fig. 9. The section pitching motion that was superimposed on this plunging motion varies with z and t as shown in Fig. 11, and the relative section angle of attack for this flapping cycle is shown in Fig. 13.

Results similar to those shown in Figs. 9–13 were obtained for 13 rectangular wings with aspect ratios ranging from 8.0 to 20.0 in steps of 1.0. Figure 14 shows the ideal propulsive efficiency for these 13 numerically optimized wings compared with the analytical solutions obtained for pure plunging and for linear washout with the minimum-power washout magnitude. At an aspect ratio of 20, the numerically optimized solution predicts an ideal propulsive efficiency in excess of 97%. For aspect ratios of 12 and above, ideal propulsive efficiencies of 90% or more are predicted for the numerically optimized solutions, and efficiencies of 95% or more are predicted for aspect ratios of 17 and higher.

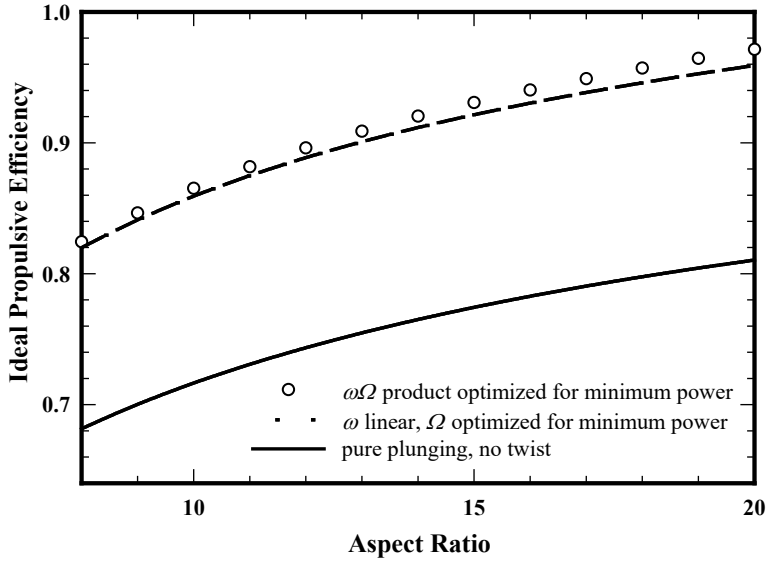

Figure 14. Propulsive efficiency as a function of aspect ratio for rectangular wings with sinusoidal flapping.

III. Conclusions

The periodic flapping motion of a bird's wing can be very complex, incorporating time-dependent spanwise variations in both twist and sweep, which are coordinated with the periodic flapping motion. Moreover, because the wing of a bird is multi-jointed and the bones and wingtip feathers are not rigid, the angular flapping rate can vary significantly across the wing semispans. Although a simple two-dimensional model is commonly used to describe the production of thrust by wing flapping, negative lift predicted during the wing upstroke has been of significant concern to many who have attempted to explain the physics associated with the flapping flight of birds in the Earth's atmosphere. One common explanation is that birds must retract their wings slightly or separate their feathers on the upstroke to reduce the detrimental effects of this negative lift. The lifting-line solutions presented here have shown that such complex flapping cycles are unnecessary for the efficient production of thrust in forward flight. For high-speed sustained flight and other flight phases where aerodynamic efficiency and endurance are of paramount importance, lifting-line theory shows that high propulsive efficiencies can be attained even with a very simple pure-plunging flapping cycle. Furthermore, the lifting-line relation for predicting the induced drag and thrust developed by wing flapping can be used for more complex flapping cycles.

One advantage of the decomposed lifting-line solution presented here is that it allows us to examine separately each of the contributing factors associated with the lift, drag, and power coefficients, even when the wing flapping motion is very complex. Another significant advantage of this quasi-steady analytical solution over commonly used numerical methods is the utility provided for optimizing wing flapping cycles. The decomposed lifting-line solution involves five time-dependent functions that could all be optimized to maximize propulsive efficiency, thrust, and/or other performance measures. The optimization study presented here was limited to the optimization of wing twist for maximum propulsive efficiency, within the constraints of sinusoidal flapping and no semispan bending.

The decomposed lifting-line solutions that are presented here show that the propulsive efficiency associated with wing flapping can be very competitive with traditional methods of aircraft propulsion. Using a pure-plunging sinusoidal flapping cycle for untwisted rectangular wings with no semispan bending, the lifting-line solution predicts ideal propulsive efficiencies in excess of 80% for wing aspect ratios near 20. It has been shown here that this propulsive efficiency can be significantly increased by using a flapping cycle composed of a combination of periodic plunging and pitching motion. For the case of time-independent plunging and twist distribution functions, a closed-form analytical solution is presented for the instantaneous amount of wing twist that requires minimum power input per unit induced thrust. Within the constraints of sinusoidal flapping, no semispan bending, and linear twist, this plunging–pitching motion increases the propulsive efficiency for a rectangular wing of aspect ratio 14 from 76.5% to 91.2%, relative to pure plunging. For this same wing planform, a further increase in ideal propulsive efficiency to 92.0% was obtained from numerical optimization of the wing twist distribution–magnitude product at each instant in time during the flapping cycle. For a rectangular wing of aspect ratio 20, this twist-optimized flapping cycle produced an ideal propulsive efficiency in excess of 97%.

The application of lifting-line theory to flapping wings is not limited to sinusoidal flapping with no semispan bending. It is likely that by allowing the angular flapping rate as well as the wing twist to vary along the wing semispan and with time during the flapping cycle, propulsive efficiencies in excess of those presented here could be attained. The decomposed lifting-line solution method presented here could be used to analyze and optimize these more complex flapping cycles. Furthermore, by using numerical lifting-line solutions, the effects of variable sweep on propulsive efficiency could be investigated as well.

References

[1]Prandtl, L., "Tragflügel Theorie," Nachricten von der Gesellschaft der Wissenschaften zu Göttingen, Geschäeftliche Mitteilungen, Klasse, 1918, pp. 451–477.

[2]Prandtl, L., "Applications of Modern Hydrodynamics to Aeronautics," NACA TR-116, June 1921.

[3]Kutta, M. W., "Auftriebskräfte in Strömenden Flüssigkeiten," *Illustrierte Aeronautische Mitteilungen*, Vol. 6, No. 133, 1902.

[4]Joukowski, N. E., "Sur les Tourbillons Adjionts," *Traraux de la Section Physique de la Societé Imperiale des Amis des Sciences Naturales*, Vol. 13, No. 2, 1906.

[5]Phillips, W. F., "Analytical Decomposition of Wing Roll and Flapping Using Lifting-Line Theory," Presented at the 31st AIAA Applied Aerodynamics Conference, San Diego, California, 24–27 June 2013.

[6]Theodorsen, T., "General Theory of Aerodynamic Instability and the Mechanism of Flutter," NACA TR-496, Dec. 1949.

[7]Phillips, W. F., "Lifting-Line Analysis for Twisted Wings and Washout-Optimized Wings," *Journal of Aircraft*, Vol. 41, No. 1, 2004, pp. 128–136.

[8]Phillips, W. F., Alley, N. R., and Goodrich, W. D., "Lifting-Line Analysis of Roll Control and Variable Twist," *Journal of Aircraft*, Vol. 41, No. 5, 2004, pp. 1169–1176.

[9]Phillips, W. F., Fugal, S. R., and Spall, R. E., "Minimizing Induced Drag with Wing Twist, Computational-Fluid-Dynamics Validation," *Journal of Aircraft*, Vol. 43, No. 2, 2006, pp. 437–444.

[10]Phillips, W. F., "Incompressible Flow over Finite Wings," *Mechanics of Flight*, 2nd ed., Wiley, Hoboken, NJ, 2010, pp. 46–94.

[11]Hunsaker, D. F., "Evaluation of an Incompressible Energy-Vorticity Turbulence Model for Fully Rough Pipe Flow", Ph. D. Dissertation, Department of Mechanical and Aerospace Engineering, Utah State University, Logan, UT, 2011.

[12]Phillips, W. F., Fowler, E. B., Hunsaker, D. F., "Energy–Vorticity Turbulence Model with Application to Flow Near Rough Surfaces," *AIAA Journal*, Vol. 51, No. 5, 2013, pp. 1211–1220.

[13]Broyden, C. G., "The Convergence of a Class of Double-rank Minimization Algorithms," *Journal of the Institute of Mathematics and Its Applications,* Vol. 6, 1970, pp. 76–90.

[14]Fletcher, R., "A New Approach to Variable Metric Algorithms," *The Computer Journal*, Vol. 13, 1970, pp. 317–322.

[15]Goldfarb, D., "A Family of Variable Metric Methods Derived by Variational Means," *Mathematics of Computation*, Vol. 24, 1970, pp. 23–16.

[16]Shanno, D. F., "Conditioning of Quasi-Newton Methods for Function Minimization," *Mathematics of Computation*, Vol. 24, 1970, pp. 647–656.